

Magnetic properties of cobalt clusters embedded in a copper matrix

Xiao Chuanyun

Chinese Center of Advanced Science and Technology (World Laboratory), P.O. Box 8730, Beijing 100080, People's Republic of China and Department of Physics, Central China Normal University, Wuhan, Hubei 430070, People's Republic of China

Yang Jinlong

Chinese Center of Advanced Science and Technology (World Laboratory), P.O. Box 8730, Beijing 100080, People's Republic of China and Center for Fundamental Physics, University of Science and Technology of China, Hefei, Anhui 230026, People's Republic of China

Deng Kaiming

Department of Applied Physics, Nanjing University of Science and Technology, Nanjing, Jiangsu 210014, People's Republic of China

Wang Kelin

Center for Fundamental Physics, University of Science and Technology of China, Hefei, Anhui 230026, People's Republic of China

(Received 15 April 1996; revised manuscript received 29 October 1996)

The magnetic properties of Co_N clusters ($N=1, 13, 19,$ and 43) embedded in copper matrix are studied using the discrete-variational local-spin-density-functional method and embedded cluster models. Single Co atom in Cu is found to be nonmagnetic, while all the rest Co clusters in Cu are still magnetic with reduced moments. Cu atoms in granular Co/Cu system reveal similar spin polarizations to Cu atoms in Co/Cu multilayers as manifested in recent x-ray magnetic circular dichroism measurements. [S0163-1829(97)03406-1]

I. INTRODUCTION

Transition-metal clusters have been the subject of widespread investigations in recent years.¹ This is not only because such clusters may serve as models for understanding localized effects in metals, but also because their intrinsic electronic, optical, magnetic, and structural properties are of fundamental importance in exploring new cluster-based materials with tailored properties.²

Many theoretical calculations and experimental measurements have been made for free cobalt clusters. Experimentally, various sizes of cobalt clusters have been generated by laser vaporization technique and their mass spectra, ionization potentials, magnetic moments, and reactivity toward small gaseous molecules have been measured.³⁻⁵ Theoretically, Khanna and Linderoth⁶ demonstrated that the magnetic properties of the Co_N clusters can be well characterized with the superparamagnetic model; Li *et al.*⁷ made a discrete-variational local-spin-density-functional (DV-LSD) study on the electronic and magnetic properties of Co_N ($N=4, 6, 13,$ and 19) with interatomic distance taken to be the bulk value; while Miura *et al.*⁸ employed the same method to study the magnetic properties of an octahedral Co_{19} and an octahedral as well as icosahedral Co_{13} clusters with optimized bond lengths. All of these studies have shown that the clusters possess enhanced magnetic moments over the bulk value and the surface atoms of the clusters are more magnetic than the inner atoms.

For most technological applications, the properties of embedded clusters are more important than free ones since they are related to the granular or island geometrical arrangements observed in granular systems, overlayers, sandwiches, and multilayers. For example, recent experimental works on non-multilayered systems demonstrated that giant magnetoresis-

tance (GMR) is not restricted to multilayered systems; it is also present in many magnetic granular systems consisting of immiscible heterogeneous elements such as Co/Cu,⁹⁻¹² Fe/Cu,¹³ Co/Ag,^{14,15} Co/Au,¹⁶ etc., wherein ferromagnetic particles are embedded in a nonmagnetic matrix and the GMR in such systems were reported to be dependent on the size of the magnetic particles, local magnetization of ferromagnetic entities and the angle that the local magnetization vector of ferromagnetic particles made with the direction of the applied field.¹³ Therefore, it is of great importance to extend our knowledge on free ferromagnetic clusters to the situations where these clusters are embedded in an environment. Comparison between the behaviors of the free and embedded clusters would contribute much to the understanding of the specific properties of these materials.

In this paper, we reported a comprehensive first-principles study on the Co_N clusters ($N=1, 13, 19,$ and 43) embedded in copper matrix in the hope to explore the influence of the Cu matrix on the magnetic moments of the Co_N clusters. To our knowledge, there are only a few theoretical studies¹⁷⁻¹⁹ devoted to such subjects to date. We chose Cu as the matrix because much work has been focused on the GMR and related magnetic properties of nonmultilayered as well as multilayered Co/Cu and Fe/Cu systems, and nanoscale Co or Fe particles can be obtained with ease in the Cu matrix. The paper is arranged as follows: the cluster models and computational parameters are described in Sec. II; our results and discussions are presented in Sec. III; finally, a summary is given in Sec. IV.

II. CLUSTER MODELS AND COMPUTATIONAL PARAMETERS

As is well known, the band theories rely on translational symmetry and are difficult to be used to treat a small particle

TABLE I. Mulliken populations, net charge, local magnetic moments (in μ_B) for atoms at different shells, and total moments of the clusters. The number of atoms for each shell is given in parentheses. The signs of the moments are given relative to the polarization of the central Co atom for all clusters.

		Charge			Net charge	Local moment			Total moment
		3d	4s	4p		3d	4s	4p	
Co ₁₃	center(1)	7.71	0.83	0.08	0.38	1.17	-0.06	0.58	27
	2nd(12)	7.48	0.91	0.64	-0.03	2.06	0.06	-0.01	
Co ₁₉	center(1)	7.67	0.53	0.01	0.79	1.72	-0.04	0.21	37
	2nd(12)	7.48	0.81	0.96	-0.25	1.91	0.04	-0.09	
	3rd(6)	7.42	0.81	0.40	0.37	2.11	-0.01	0.05	
Co ₄₃	center(1)	7.27	0.60	1.43	-0.30	1.66	-0.08	-0.14	91
	2nd(12)	7.40	0.55	1.28	-0.23	1.77	-0.04	0.03	
	3rd(6)	7.35	0.85	1.24	-0.44	2.10	-0.05	-0.06	
	4th(24)	7.39	0.83	0.53	0.25	2.27	0.05	0.04	
Cu ₄₃	center(1)	9.76	0.21	0.76	0.27	0.00	0.00	0.00	-3
	2nd(12)	9.81	0.52	1.16	-0.49	-0.01	0.00	-0.03	
	3rd(6)	9.86	0.60	0.73	-0.19	0.00	0.00	-0.13	
	4th(24)	9.88	0.71	0.13	0.28	0.00	-0.07	0.00	
CoCu ₄₂	center(1)	7.39	0.10	0.57	0.94	0.06	0.00	0.00	-1
	2nd(12)	9.81	0.55	1.25	-0.61	0.00	0.00	-0.02	
	3rd(6)	9.86	0.62	0.62	-0.10	0.00	0.00	-0.05	
	4th(24)	9.88	0.71	0.13	0.28	0.00	-0.02	0.00	
Co ₁₃ Cu ₃₀	center(1)	7.48	0.65	0.39	0.48	1.15	-0.07	0.24	23
	2nd(12)	7.42	0.52	1.30	-0.24	1.78	0.00	0.00	
	3rd(6)	9.83	0.71	1.02	-0.56	0.04	-0.05	-0.13	
	4th(24)	9.87	0.70	0.19	0.24	0.02	0.03	0.00	
Co ₁₉ Cu ₂₄	center(1)	7.43	0.63	0.84	0.10	1.20	-0.08	0.03	35
	2nd(12)	7.43	0.54	1.30	-0.27	1.70	-0.03	0.00	
	3rd(6)	7.37	0.75	1.04	-0.16	2.17	0.00	0.10	
	4th(24)	9.86	0.73	0.25	0.17	0.03	0.00	-0.02	
Co ₄₃ Cu ₁₂	center(1)	7.25	0.72	1.70	-0.67	1.86	-0.07	-0.09	81
	2nd(12)	7.44	0.50	1.25	-0.19	1.46	-0.05	0.06	
	3rd(6)	7.40	0.75	0.97	-0.12	2.05	-0.08	-0.10	
	4th(24)	7.41	0.74	0.66	0.19	2.12	0.00	0.02	
	5th(12)	9.85	0.83	0.39	-0.07	0.03	-0.06	-0.06	

of a metal in a host where a very large supercell is required. Since the magnetic property of the granular particle in a matrix is determined dominantly by its local environment, we can conveniently treat the local problem with a first-principles embedded cluster method, which considers several shells of host atoms surrounding the impurity particle as a cluster, with the effect of the rest host atoms on the cluster taken into account in an embedded scheme, to simulate the environment of the impurity in bulk host. In the present study, we have considered several octahedral (O_h) clusters of 43 or 55 atoms, namely, $\text{Co}_N\text{Cu}_{43-N}$ ($N=1, 13, 19$) and $\text{Co}_{43}\text{Cu}_{12}$ which consist of a central Co atom coordinated by several shells of Co or Cu atoms in fcc geometry, to represent the granular particles of Co_N ($N=1, 13, 19$, and 43) in fcc Cu matrix. The geometrical parameters for these clusters are chosen as follows. The Co-Cu distance is taken to be the average of the bulk Co and Cu for all clusters. The Co-Co distances for the O_h $\text{Co}_{13}\text{Cu}_{30}$ and O_h $\text{Co}_{19}\text{Cu}_{24}$ clusters are taken to be those optimized by Miura *et al.* for free O_h Co_{13} and O_h Co_{19} clusters, respectively, while it assumes the bulk value for the O_h $\text{Co}_{43}\text{Cu}_{12}$ cluster. In our embedded scheme, the 43- or 55-atom clusters are emerged in the po-

tential field of several hundred of Cu atoms of the external part of the crystal, so as to diminish spurious effects of simulating the solid by cluster models.^{19,20}

We used the same DV-LSD method as Li *et al.*⁷ and Miura *et al.*⁸ in the calculations for our embedded clusters. This method has been applied successfully to study the magnetic and structural properties of many metal clusters and bulk systems.¹⁹⁻²¹ As it has been described in detail elsewhere,^{22,20} no further description will be given here. Briefly, the DV-LSD method is a kind of molecular orbital calculation method based on the LSD theory.²³ The electronic structures of the clusters are obtained by solving the Kohn-Sham²³ equations self-consistently in the spin-polarized scheme and the magnetic properties of the clusters can be obtained via the Mulliken spin population analysis. The self-consistent charge (SCC) scheme²² and the von Barth-Hedin²⁴ exchange-correlation potential parametrized by Moruzzi *et al.*²⁵ are adopted in present calculation. In the embedded cluster scheme, the charge density of the embedding atoms that penetrates the cluster region is added to the cluster density to construct the Kohn-Sham Hamiltonian. The numerical atomic orbitals are used as the variational

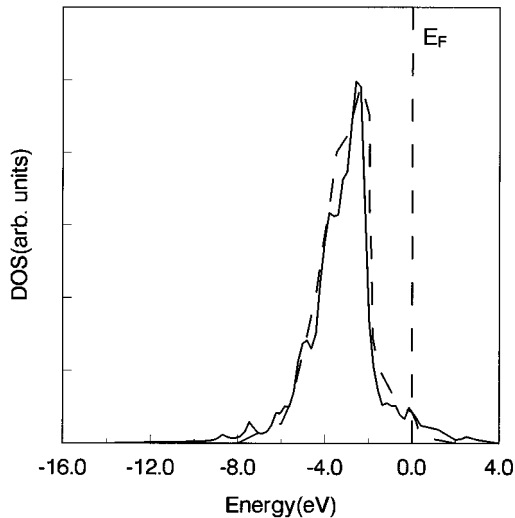


FIG. 1. Comparison of calculated DOS (solid curve) for Cu_{43} cluster with experimental valence band spectrum (dashed) for bulk Cu.

basis set to construct the molecular orbitals, which consists of the $3d$, $4s$, and $4p$ orbitals for both Co and Cu atoms of the clusters, with the core orbitals ($1s$ - $3p$) of the cluster atoms and all orbitals of the embedding atoms treated as frozen after the first iteration cycle. Using about 400 sampling points around each atomic site of the clusters in the numerical integrations, we achieved sufficient convergence in the SCC process. In recent years, the inclusion of the gradient corrections to the LSD functionals has led to excellent results for the binding energies of molecules and solids,²⁶⁻²⁸ but no improvement on the magnetic moment has been made as compared with experiments.²⁶ In present study, we have not considered the nonlocal corrections.

III. RESULTS AND DISCUSSIONS

We first studied the embedded O_h Cu_{43} cluster with bulk interatomic spacing. By starting with an initial magnetic configuration of the Cu atoms and performing a spin-polarized self-consistent calculation, we obtained an approximately bulklike paramagnetic state (see Table I) for Cu_{43} cluster. The very small magnetic moment per atom (about $0.06 \mu_B/\text{atom}$) can be explained simply as the requirements of the odd number of electrons in the cluster and the size and geometry of the cluster. Figure 1 shows the density of states (DOS) for this cluster, which is obtained by a Lorentzian broadening of the discrete energy levels and a summation over them. The broadening width used in this study is 0.2 eV for all DOS's. As seen from the figure, our DOS well reproduces the valence band spectrum obtained by an x-ray photoemission spectroscopy study²⁹ for bulk Cu. This cluster, therefore, seems to be reasonable to represent the bulk Cu for dealing with the local problems in it.

Now let's examine the influence of the Cu matrix on the magnetic properties of various sizes of Co clusters with our embedded cluster models. Our main results are presented in Table I and in Figs. 2-4.

For comparison, Table I also includes our results for free O_h Co_N ($N=13, 19$, and 43) clusters, the bond lengths of

which are taken to be the same as those in corresponding embedded clusters. As seen in Table I, we obtained the same values of the total magnetic moments as Miura *et al.*⁸ for both the Co_{13} and the Co_{19} clusters. Li *et al.*⁷ have obtained a similar moment of $27.43 \mu_B$ for their O_h Co_{13} cluster with the bulk bond length. The small nonintegral difference in Li's result from ours for the O_h Co_{13} cluster arises not from their longer bond length, but from their thermal smearing of the occupation of the levels used to accelerate the iteration convergence. For the O_h Co_{19} cluster, Li *et al.*⁷ obtained a moment of $41 \mu_B$, which is larger by $4 \mu_B$ than the result of Miura *et al.* and ours, indicating the significant bond-length dependence of the cluster moment. For the free Co_{43} cluster, we obtained a total moment of $91 \mu_B$, or $2.12 \mu_B/\text{atom}$, which is close to the experimental value of $2.08 \mu_B/\text{atom}$ obtained by using the superparamagnetic model for small cobalt clusters.⁶

We start with discussing the local magnetism of single Co impurity in Cu matrix, which has been a subject of extensive theoretical and experimental investigations. Podloucky *et al.*^{30,31} have made self-consistent LSD calculations on the magnetic moment of Co impurity in dilute CoCu alloy with the Korringa-Kohn-Rostoker (KKR) Green's function method in two schemes. In the single-site calculation (SSC) scheme,³⁰ they found Co to be nonmagnetic. In an improved impurity-cluster calculation (ICC) scheme,³¹ however, they obtained a local moment of $0.96 \mu_B$ for isolated Co impurity. More recently, Stefanou, and Papanikolaou³² studied this problem by performing self-consistent LSD calculations for all the $3d$ elements embedded in jellium host and concluded that single Co should be nonmagnetic in Cu. As seen in Table I, our cluster model calculation shows that the magnetic moment of single Co in Cu is almost completely quenched with a very small moment of $0.06 \mu_B$, which is in agreement with the result of Stefanou and Papanikolaou and the SSC result of Podloucky *et al.* and with the anomalous Hall-effect measurement made by Kramer and Bergmann³³ which indicated that Co impurities in disordered Cu films are nonmagnetic. Since we don't know the calculation details of the KKR methods of Podloucky *et al.*,^{30,31} it is hard for us to comment on the discrepancy between our result and the ICC result of them. By comparing the magnetic moments and the Mulliken populations for the Cu atoms at corresponding shells in the Cu_{43} and the CoCu_{42} clusters, we can see that Co has influence mainly on the first two shells of neighboring Cu atoms.

While the magnetism of single Co in Cu is completely quenched, larger Co clusters in Cu matrix are still magnetic with reduced moments as compared with the corresponding free ones (see Table I). The reduction ratios for the magnetic moments of the Co_N ($N=1, 13, 19$, and 43) clusters in Cu are found to be 98, 16, 6, and 10 %, respectively, which do not decrease monotonically with the increasing size of Co clusters. Since the reduced moments for the CoCu_{42} , $\text{Co}_{13}\text{Cu}_{30}$, and $\text{Co}_{43}\text{Cu}_{12}$ clusters are mostly from the outermost shell of Co atoms, we can correlate their reduction ratios to the surface-to-volume ratio of Co particles, or the ratio of the number of surface Co atoms to the total number of Co atoms in the Co cluster. In fact, the surface-to-volume ratio for Co in CoCu_{42} , $\text{Co}_{13}\text{Cu}_{30}$, and $\text{Co}_{43}\text{Cu}_{12}$ clusters are, respectively, 100, 92, and 56 %, in just the same se-

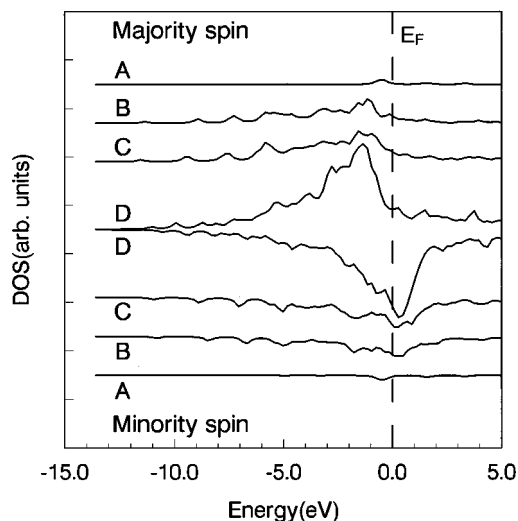


FIG. 2. Total density of states for Co particles in (A) CoCu_{42} , (B) $\text{Co}_{13}\text{Cu}_{30}$, (C) $\text{Co}_{19}\text{Cu}_{24}$, and (D) $\text{Co}_{43}\text{Cu}_{12}$ clusters. E_F denotes the Fermi level.

quence as the reduction ratios for the moments of these Co clusters. For the $\text{Co}_{19}\text{Cu}_{24}$ cluster, the reduced moment comes mostly from the next outermost shell of Co atoms and the outermost shell of Co atoms have an even larger moment compared with free Co_{19} . This is because in Co_{19} there are only six Co atoms at the outermost shell and thus parts of Co atoms at the next outermost shell are exposed to the Cu atoms and act as the surface atoms. With this consideration in mind, we can say that the reduction ratio for the moment of Co_{19} in Cu is also proportional to the surface-to-volume ratio of the cluster. It follows that clusters of a specific size but different symmetric geometries may show very different reduction ratios in the magnetic moments because of very different surface-to-volume ratios if there were a way to embed them in the same matrix. This conclusion can be helpful for material design. Another exception for the $\text{Co}_{19}\text{Cu}_{24}$ cluster is that the interactions between the outermost shell of

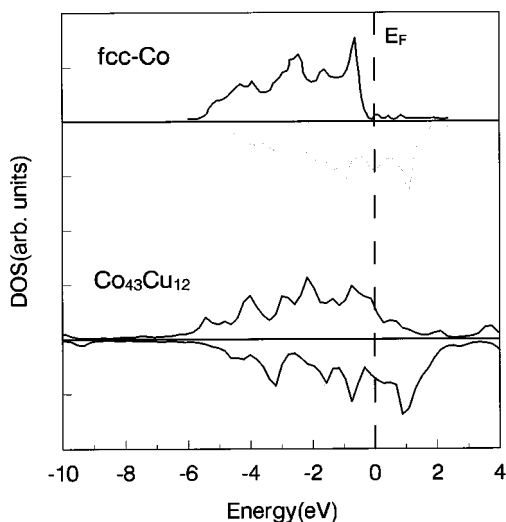


FIG. 3. Comparison of the density of states for bulk fcc Co and the local density of states for central Co atom of $\text{Co}_{43}\text{Cu}_{12}$ clusters.

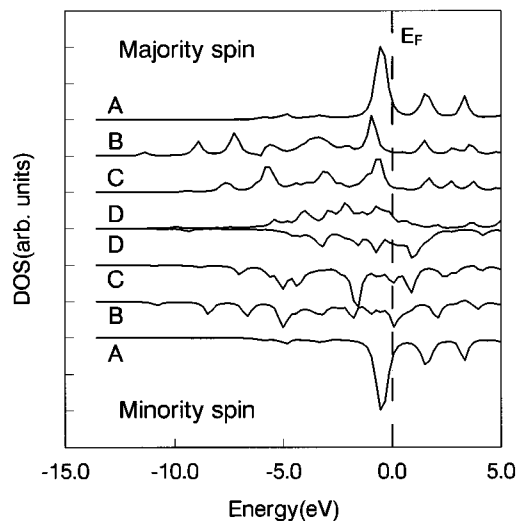


FIG. 4. Local density of states for central Co atom of (A) CoCu_{42} , (B) $\text{Co}_{13}\text{Cu}_{30}$, (C) $\text{Co}_{19}\text{Cu}_{24}$, and (D) $\text{Co}_{43}\text{Cu}_{12}$ clusters.

Co atoms and the nearest shell of Cu atoms are ferromagnetic in this cluster while such interactions are antiferromagnetic in all the rest clusters. This ferromagnetic coupling results in an enhanced moment for the outermost shell of Co atoms in $\text{Co}_{19}\text{Cu}_{24}$ compared with the free Co_{19} .

It is interesting to note from Table I that the moments for the outermost shell of Co atoms in the Co_{13} and the Co_{19} clusters are depressed to a greater extent when surrounded by ferromagnetic Co atoms than by nonmagnetic Cu atoms. This can be seen by comparing the magnetic moments for free Co_{13} and Co_{19} clusters with $\text{Co}_{13}\text{Cu}_{30}$ or $\text{Co}_{19}\text{Cu}_{24}$, and with corresponding portions of free Co_{43} cluster which can be viewed as $\text{Co}_{13}\text{Co}_{30}$ or $\text{Co}_{19}\text{Co}_{24}$, and the practical magnetic depression by Co should be even larger since the Co-Co distance used for the Co_{13} and Co_{19} fragments in the Co_{43} cluster (bulk value) is longer than those for the corresponding Co_{13} and Co_{19} clusters (optimized values) and thereby overestimated their magnetic moments. As the Co-Cu distance we take for the $\text{Co}_{13}\text{Cu}_{30}$ and $\text{Co}_{19}\text{Cu}_{24}$ clusters (4.78 a.u.) is only slightly longer than the Co-Co distance for Co_{43} cluster (4.73 a.u.), it's hard to attribute this result to the difference in Co-Co and Co-Cu bond lengths. We argue that this result may be due to the difference in $\text{Co}3d\text{-Co}3d$ and $\text{Co}3d\text{-Cu}3d$ hybridizations.

Another interesting result is that the magnetic moment for the central Co atom of the $\text{Co}_{43}\text{Cu}_{12}$ cluster is even larger than that for the central Co atom of free Co_{43} cluster. Similar anomalous enhancement of magnetic moments has also been shown for Fe atoms at the center of Fe clusters embedded in Cr (Ref. 17) or Cu (Ref. 19) matrices, and for Fe atoms in the middle of the Fe slab of the Fe/Cr multilayers,^{34,35} but no explanation has been given.

Our results are somewhat different from the cases of carbonyl or helium ligated Ni clusters,^{36,37} where both the LSD calculations and experimental magnetization studies indicated that the magnetic moments of the Ni atoms at the surface of various sizes of Ni_N clusters (N up to 147) are almost completely quenched by the surrounding carbonyl or helium ligands, while the innercore Ni atoms are relatively unaffected.

Recently, Samant *et al.*³⁸ and Pizzini *et al.*³⁹ made x-ray magnetic circular dichroism (XMCD) measurements on Co/Cu and Fe/Cu multilayers at the *K* edge of copper, which allows to probe the induced spin polarizations on the Cu atoms and to distinguish between Cu3*d* and Cu4*p* states. According to these experimental measurements, the 3*d* electrons of Cu atoms are polarized parallel to the 3*d* moment of Co, whereas the 4*p* of Cu are antiparallel. As seen from Table I, the calculated magnetizations for Cu atoms in all embedded clusters we considered show the similar spin polarizations to these experimental observations. This result and the above-mentioned moment enhancement shared by both the granular systems and the multilayers are consistent with the original suggestion of Berkowitz *et al.*⁹ and Xiao *et al.*¹⁰ that granular magnetic solids might be giant-magneto-resistive in the similar mechanism to multilayers.

Figure 2 shows the total density of states (DOS) for the Co clusters in Cu matrix. The exchange splittings are estimated to be 0.0 eV for single Co, 1.2 eV for Co₁₃, and 1.6 eV for both Co₁₉ and Co₄₃ clusters in Cu. By a KKR or augmented spherical wave (ASW) band structure calculation, Moruzzi *et al.* obtained an exchange splitting for bulk fcc Co to be 1.5 (Ref. 25) or 1.7 eV (Ref. 40), respectively, in good agreement with our results for Co₁₉ and Co₄₃ clusters in Cu.

In Fig. 3 we present the DOS of an ASW band structure calculation for bulk fcc Co.⁴⁰ Compared with the total DOS for the Co clusters in Cu (see Fig. 2), we see little similarity between them. Since the central atom of a cluster is the most representative of the bulk counterpart, we expect that the local DOS for the central Co atom of the Co clusters in Cu matrix would show some similarity to the bulk DOS of fcc Co and the similarity would increase with increased size of the cluster. Figure 4 is the local DOS for the central Co atom of the Co clusters in Cu matrix. One finds that the local DOS for the central Co atom of Co₄₃ cluster in Cu is very similar to the bulk DOS of fcc Co in the band width and corresponding peaks, as is separately shown in Fig. 3 for clearer comparison.

Finally, we discuss the Mulliken populations for the embedded clusters as presented in Table I. Considerable charge transfer exists in all of these clusters. Since the electronegativity for Cu is close to that for Co, it is expected that elec-

trons may transfer either from Co to Cu or from Cu to Co, depending upon the specific environment of the atoms. For the CoCu₄₂ and Co₄₃Cu₁₂ clusters, there is less than one electron migrating from Co4*s* to Cu4*p*. However, about 2.4*e* and 4.1*e* charges are found to transfer from Cu3*d*4*s* to Co3*d*4*p* in Co₁₃Cu₃₀ and Co₁₉Cu₂₄ clusters, respectively. In addition, there is also considerable charge redistribution between different shells of Co atoms and among different atomic orbitals of the same atom in all embedded clusters. These results are different from those of Fe particles in Cr and Cu matrices,^{17,19} where small charge transfer is found between Fe and Cr or Cu.

IV. SUMMARY

In this paper, we have performed a comprehensive first-principles study on the magnetic properties of Co_{*N*} clusters (*N*=1, 13, 19, and 43) embedded in copper matrix. Single Co atom in Cu matrix is found to be nonmagnetic, which is in agreement with previous theoretical studies^{30,32} and abnormal Hall-effect measurement,³³ while all of the rest Co clusters in Cu matrix are still magnetic with reduced moments. The reduction ratio does not decrease monotonically with the increasing size of Co clusters and is correlated to the surface-to-volume ratio of the Co clusters. It is found that the central Co atom of Co clusters has an enhanced moment when embedded in Cu matrix. Similar enhancement in the magnetic moment was also found for the central Fe atoms of Fe clusters embedded in Cr (Ref. 17) and Cu (Ref. 19) and for the Fe atoms in the middle of the Fe slab of the Fe/Cr multilayers.^{34,35} The Cu atoms in granular Co/Cu system is found to have similar spin polarizations to Cu atoms in Co/Cu multilayers.^{38,39} Finally, significant charge transfers are found both between different shells of Co and Cu atoms and between different orbitals of the same atom.

ACKNOWLEDGMENTS

This work was supported by the National Natural Science Foundation of China and the Foundations of the Chinese Academy of Science and the National Education Commission for the Returned Chinese Scholars.

¹For a review, see *Proceedings of the Seventh International Meeting on Small Particles and Inorganic Clusters*, Kobe, Japan, 1994 [Surf. Rev. Lett. **3** (1996)].

²S.N. Khanna and P. Jena, Phys. Rev. Lett. **69**, 1664 (1992); Phys. Rev. B **51**, 13 705 (1995).

³M.D. Morse, M.E. Geusic, J.R. Heath, and R.E. Smalley, J. Chem. Phys. **83**, 2293 (1985).

⁴S. Yang and M.B. Knickelbein, J. Chem. Phys. **93**, 1533 (1990).

⁵J.P. Bucher, D.C. Douglass, and L.A. Bloomfield, Phys. Rev. Lett. **66**, 3052 (1991).

⁶S. N. Khanna and S. Linderoth, Phys. Rev. Lett. **67**, 742 (1991).

⁷Zhi-qiang Li and Bing-lin Gu, Phys. Rev. B **47**, 13 611 (1993).

⁸K. Miura, H. Kimura, and S. Imanaga, Phys. Rev. B **50**, 10 335 (1994).

⁹A.E. Berkowitz *et al.*, Phys. Rev. Lett. **68**, 3745 (1992).

¹⁰J.Q. Xiao, J.S. Jiang, and C.L. Chien, Phys. Rev. Lett. **68**, 3749 (1992).

¹¹B.J. Hickey, M.A. Howson, S.O. Musa, and N. Wisser, Phys. Rev. B **51**, 667 (1995).

¹²R.H. Yu, X.X. Zhang, J. Tejada, M. Knobel, P. Tiberto, and P. Allia, J. Phys. Condens. Matter **7**, 4081 (1995).

¹³M. Eilon, J. Ding, and R. Street, J. Phys. Condens. Matter **7**, 4921 (1995).

¹⁴J.A. Barnard *et al.*, J. Magn. Magn. Mater. **114**, L230 (1992).

¹⁵H. Sato, Y. Kobayashi, Y. Aoki, and H. Yamamoto, J. Phys. Condens. Matter **7**, 7053 (1995).

¹⁶S.M. Thompson *et al.*, Philos. Mag. B **68**, 923 (1993).

¹⁷A. Vega, L.C. Balbás, J. Dorantes-Dávila, and G.M. Pastor, Phys. Rev. B **50**, 3899 (1994).

¹⁸Zhi-qiang Li *et al.*, J. Phys. Condens. Matter **7**, 7367 (1995).

- ¹⁹D. Guenzburger and D.E. Ellis, *Phys. Rev. B* **52**, 13 390 (1995).
- ²⁰D. Guenzburger and D.E. Ellis, *Phys. Rev. B* **45**, 285 (1992).
- ²¹Yang Jinlong, Xiao Chuanyun, Xia Shangda, and Wang Kelin, *Phys. Rev. B* **48**, 12 155 (1993).
- ²²D.E. Ellis and G.S. Painter, *Phys. Rev. B* **2**, 2887 (1970).
- ²³W. Kohn and L.J. Sham, *Phys. Rev. A* **140**, 1133 (1965).
- ²⁴V. von Barth and L. Hedin, *J. Phys. C* **5**, 1629 (1972).
- ²⁵V.L. Moruzzi, J.F. Janak, and A.R. Williams, *Calculated Electronic Properties of Metals* (Pergamon, New York, 1978).
- ²⁶D.J. Singh, W.E. Pickett, and H. Krakauer, *Phys. Rev. B* **43**, 11 628 (1991).
- ²⁷F.W. Kutzler and G.S. Painter, *Phys. Rev. B* **45**, 3236 (1992).
- ²⁸J.P. Perdew *et al.*, *Phys. Rev. B* **46**, 6671 (1992).
- ²⁹H. Höchst, P. Steiner, and S. Hüfner, *Z. Phys. B* **38**, 201 (1980).
- ³⁰R. Podloucky, R. Zeller, and P.H. Dederichs, *Phys. Rev. B* **22**, 5777 (1980).
- ³¹P. J. Braspenning, R. Zeller, A. Lodder, and P.H. Dederichs, *Phys. Rev. B* **29**, 703 (1984).
- ³²N. Stefanou and N. Papanikolaou, *J. Phys. Condens. Matter* **3**, 3777 (1991).
- ³³I. Kramer and G. Bergmann, *Z. Phys. B* **47**, 321 (1982).
- ³⁴Z.P. Shi, P.M. Levy, and J.L. Fry, *Phys. Rev. Lett.* **69**, 3678 (1992).
- ³⁵J-h. Xu and A.J. Freeman, *Phys. Rev. B* **47**, 165 (1993).
- ³⁶D. A. van Leeuwen *et al.*, *Phys. Rev. Lett.* **73**, 1432 (1994).
- ³⁷G. Paccioni, S.C. Chung, S. Krüger, and N. Rösch, *Chem. Phys.* **184**, 125 (1994).
- ³⁸M.G. Samant *et al.*, *Phys. Rev. Lett.* **72**, 1112 (1994).
- ³⁹S. Pizzini *et al.*, *Phys. Rev. Lett.* **74**, 1470 (1995).
- ⁴⁰P.M. Marcus and V.L. Moruzzi, *Solid State Commun.* **55**, 971 (1985).